AD-A070 484 MARYLAND UNIV COLLEGE PARK DEPT OF PHYSICS AND ASTRONOMY F/G 20/9
INFLUENCE OF AXIAL ENERGY SPREAD ON THE NEGATIVE-MASS INSTABILI--ETC(U)
1978 H UHM, R C DAVIDSON N00014-75-C-0309
UNCLASSIFIED PUB-78-020 NL

| OF |
AD A070484

END
DATE FILMED
7-79
DDC

PREPRINT #808P001

Influence of Axial Energy Spread on the Negative-Mass Instability in a Relativistic Nonneutral E-Layer

Hwan-sup Uhm
Department of Physics and Astronomy
University of Maryland, College Park, Maryland 20742

and

Ronald C. Davidson*
Division of Magnetic Fusion Energy
Energy Research and Development Administration
Washington, D. C. 20545

Physics Publication Number 78-020
1978

Work on this report was supported
by ONR Contract N00014-75-C-0309
and/or N00014-67-A-0239
monitored by NRL Code 6702.

UNIVERSITY OF MARYLAND
DEPARTMENT OF PHYSICS AND ASTRONOMY
COLLEGE PARK, MARYLAND

*On leave of absence from the University of Maryland, College Park, Md.

DDC PROCESSING DATA

PHOTOGRAPH

THIS SHEET

RETURN TO DDA-2 FOR FILE

II
LEVEL

1
INVENTORY

AD A070484
DDC ACCESSION NUMBER

Preprint 808P001, Physics Pub. 78-020
DOCUMENT IDENTIFICATION

DISTRIBUTION STATEMENT A
Approved for public release;
Distribution Unlimited

DISTRIBUTION STATEMENT

Accession For
NTIS GRA&I
DDC TAB
Unannounced
Justification
By
Distribution/
Availability Codes
Dist. | Avail and/or special
A

DISTRIBUTION STAMP

DDC
RECEIVED
JUN 28 1979
D

DATE ACCESSIONED

79 06 27 300

DATE RECEIVED IN DDC

PHOTOGRAPH THIS SHEET

RETURN TO DDA-2

Work on this report was supported
by ONR Contract N00014-75-C-0309
and/or N00014-67-A-0239
monitored by NRL Code 6702.

INFLUENCE OF AXIAL ENERGY SPREAD ON THE NEGATIVE-MASS INSTABILITY IN A RELATIVISTIC NONNEUTRAL E-LAYER

Hwan-sup Uhm
Department of Physics and Astronomy
University of Maryland, College Park, Maryland 20742

and

Ronald C. Davidson*
Division of Magnetic Fusion Energy
Energy Research and Development Administration
Washington, D. C. 20545

This paper investigates the influence of an axial energy spread on the negative-mass instability in a relativistic nonneutral E-layer aligned parallel to a uniform axial magnetic field $B_0\hat{e}_z$. The stability analysis is carried out within the framework of the linearized Vlasov-Maxwell equations. It is assumed that the E-layer is thin with radial thickness (2a) much smaller than the mean radius (R_0), and that $\nu/\gamma_0 \ll 1$, where ν is Budker's parameter and $\gamma_0 mc^2$ is the mean electron energy. Stability properties are investigated for the choice of electron distribution function in which all electrons have the same value of canonical angular momentum ($P_\theta = P_0 = \text{const.}$) and a step-function distribution in axial momentum p_z. The negative-mass growth rate is calculated including the important stabilizing influence of axial energy spread (ΔE), and it is shown that a modest energy spread ($\Delta E/\gamma_0 mc^2 \lesssim$ a few percent) is sufficient to stabilize perturbations with axial wavenumber satisfying $k^2 R_0^2 \gtrsim 1$.

*On leave of absence from the University of Maryland, College Park, Md.

I. INTRODUCTION

In recent years, the properties of relativistic electron rings and E-layers, contained in a mirror or uniform magnetic field, have been studied experimentally in connection with plasma confinement schemes such as Astron[1,2], single-stage magnetic mirrors[3,4], and electron ring accelerators[5-11]. One of the most basic instabilities that characterizes relativistic electron rings and E-layers is the negative-mass instability[8-16]. The influence of a spread in canonical angular momentum on this instability has been extensively investigated in the literature[12,14,16]. The present paper examines the equilibrium and negative-mass stability properties of a relativistic nonneutral E-layer within framework of the linearized Vlasov-Maxwell equations[17], including the important influence of an axial energy spread. Recent experimental observations[8] indicate that perturbations with finite axial wavenumber are significantly stabilized by a small axial energy spread.

The present analysis is carried out for an infinitely long E-layer aligned parallel to a uniform magnetic field $B_0 \hat{e}_z$ [Fig. 1]. Equilibrium and stability properties are calculated for the specific choice of electron distribution function [Eq. (8)].

$$f_e^0(H,P_\theta,P_z) = \frac{n_0 R_0}{2\pi\Delta(2\gamma_0 m)^{1/2}}\,\delta(P_\theta-P_0)\Theta(\Delta^2-p_z^2)\,\frac{\Theta(\hat{\gamma}mc^2-U)}{(\hat{\gamma}mc^2-U)^{1/2}} \quad ,$$

where H is the energy, P_θ is the canonical angular momentum, p_z is the axial momentum, $\Theta(x)$ is the Heaviside step function, $U \equiv H + e\bar{\phi}_0 - p_z^2/2\gamma_0 m$ is an effective energy variable, and n_0, R_0, Δ, γ_0, $\hat{\gamma}$ and $\bar{\phi}_0$ are constants. Equilibrium properties are examined in Section II. One of the important features of the equilibrium analysis is that the equilibrium distribution

function in Eq. (8) corresponds to a sharp-boundary density profile with uniform axial temperature (Fig. 2). Stability properties are investigated in Sections III and IV, including the important influence of an axial energy spread. The stability analysis is fully electromagnetic and assumes that the positive ions can be treated as a fixed background ($m_i \to \infty$) on the time scales of interest.

Introducing the geometric factor g [Eq. (44)] which is a transcendental function of the eigenfrequency ω and axial wavenumber k, we obtain the dispersion relation [Eq. (56)]

$$(\omega-\ell\omega_c)^2 = -\frac{c^2}{R_0^2}\left[\frac{\nu}{\gamma_0}\frac{g\omega_c}{\omega}(\mu\ell^2-k^2R_0^2) - 2k^2R_0^2\frac{\Delta E}{\gamma_0 mc^2}\right].$$

Here ν is Budker's parameter, $\Delta E=\Delta^2/2\gamma_0 m$ is the axial energy spread, ℓ is the azimuthal harmonic number, $\omega_c=eB_0/\gamma_0 mc$ is the electron cyclotron frequency, and $\mu=\omega_c^2/\omega_r^2 - 1/\gamma_0$ is defined in Eq. (51). A detailed numerical analysis of the dispersion relation [Eq. (56)] is carried out in Section IV. It is found that the axial energy spread (ΔE) has a strong stabilizing influence on the negative-mass instability, particularly when the perturbations have sufficiently large axial wavenumber with $k^2R_0^2 \gtrsim 1$ (Sec. IV).

As a check on the dispersion relation given in Eq. (56), it is instructive to consider the limit of an ultrarelativistic ($\gamma_0 \gg 1$), infinitisimally thin ($a/R_0 \to 0$) E-layer, with negligibly small equilibrium self fields ($\mu \simeq 1$) and axial energy spread ($\Delta E=0$). In this case, Eq. (56) can be expressed as

$$(\omega-\ell\omega_c)^2 = -(c^2/R_0^2)[(\ell^2-k^2R_0^2)(\nu/\gamma_0)g\omega_c/\omega]$$

which is identical to the result obtained by Briggs and Neil[14] within the framework of a macroscopic sheet model.

II. EQUILIBRIUM THEORY

As illustrated in Fig. 1, the equilibrium configuration consists of a relativistic nonneutral E-layer that is infinite in axial extent and aligned parallel to a uniform applied magnetic field $B_0\hat{e}_z$. The mean radius and radial thickness of the E-layer are denoted by R_0 and 2a, respectively. The mean motion of the E-layer is in the azimuthal direction, and the applied magnetic field provides radial confinement of the electrons. As shown in Fig. 1, cylindrical polar coordinates (r,θ,z) are introduced. The following are the main assumptions[16] pertaining to the equilibrium configuration:

(a) Equilibrium properties are independent of z ($\partial/\partial z=0$) and azimuthally symmetric ($\partial/\partial\theta=0$) about the z-axis.

(b) The positive ions form an immobile ($m_i\to\infty$), partially neutralizing background. It is assumed that the equilibrium ion density $n_i^0(r)$ can be expressed as

$$n_i^0(r)=fn_e^0(r) \ , \tag{1}$$

where f=const. is the fractional charge neutralization, and $n_e^0(r)$ is the electron density.

(c) The spread in radial and axial momentum of the electrons is small in comparison with the mean azimuthal momentum, i.e.,

$$\frac{a}{R_0} << \frac{\Delta}{\gamma_0 mc} << 1 \tag{2}$$

where Δ is the characteristic spread in axial momentum, $\gamma_0 mc^2$ is the azimuthal electron energy at $r=R_0$, and the half-thickness a is related to the spread in radial momentum by Eq. (18).

(d) The electron motion is generally relativistic, and the mean equilibrium motion of the E-layer is in the azimuthal direction, i.e.,

$$\int d^3p \, \underset{\sim}{v} \, f_e^0(\underset{\sim}{x},\underset{\sim}{p}) = n_e^0(r) V_\theta^0(r) \hat{\underset{\sim}{e}}_\theta \ ,$$

where $V_\theta^0(r)$ is the mean azimuthal velocity of an electron fluid element, and $\hat{\underset{\sim}{e}}_\theta$ is a unit vector in the θ-direction.

(e) It is further assumed that

$$\frac{\nu}{\gamma_0} << 1 \ , \tag{3}$$

where $\nu = N_e e^2/mc^2$ is Budker's parameter,

$$N_e = 2\pi \int_{R_1}^{R_2} dr \, r n_e^0(r) \tag{4}$$

is the number of electrons per unit axial length of the E-layer, c is the speed of light in vacuo, -e and m are the charge and rest mass, respectively, of an electron. In Eq. (4), R_1 and R_2 denote the inner and outer radii, respectively, of the E-layer.

Central to a description of steady-state Vlasov equilibria are the single-particle constants of the motion in the equilibrium field configuration. For azimuthally symmetric equilibria with $\partial/\partial z = 0$, there are <u>three</u> single-particle constants of the motion. These are the total energy H,

$$H = (m^2c^4 + c^2p^2)^{1/2} - e\phi_0(r) \ , \tag{5}$$

the canonical angular momentum P_θ,

$$P_\theta = r[p_\theta - (e/c)A_0(r)] \ , \tag{6}$$

and the axial canonical momentum P_z,

$$P_z = p_z \ , \tag{7}$$

where use has been made of assumption (d). In Eqs. (5)-(7), lower case p denotes mechanical momentum, $\phi_0(r)$ is the electrostatic potential for the equilibrium radial self-electric field [$E_r^0(r) = -\partial\phi_0/\partial r$], and $A_0(r)$ is the θ-component of the equilibrium vector potential [$B_z(r) = r^{-1}(\partial/\partial r)(rA_0)$]. Any distribution function that is a function only of the single-particle constants of the motion satisfies the steady-state Vlasov equation. For present purposes, we consider the equilibrium distribution function

$$f_e^0(H,P_\theta,P_z) = \frac{n_0 R_0}{2\pi\Lambda(2\gamma_0 m)^{1/2}}\,\delta(P_\theta - P_0)\,\Theta(\Lambda^2 - p_z^2) \cdot \frac{\Theta(\hat{\gamma}mc^2 - U)}{(\hat{\gamma}mc^2 - U)^{1/2}} \ , \tag{8}$$

where n_0 is electron density at $r=R_0$, Λ, P_0 and $\hat{\gamma}$ are constants, and $\Theta(x)$ is the Heaviside step function defined by

$$\Theta(x) = \begin{cases} 0 \ , & x<0 \ , \\ 1 \ , & x>0 \ . \end{cases} \tag{9}$$

In Eq. (8), the energy variable U is defined by

$$U = H + e\bar{\phi}_0 - p_z^2/2\gamma_0 m \ , \tag{10}$$

where $\bar{\phi}_0$ is the electrostatic potential at the mean radius R_0, i.e., $\bar{\phi}_0 = \phi_0(R_0)$. Note that U is a single-particle constant of the motion since it is constructed from a linear combination of H and p_z^2.

For a thin E-layer equilibrium consistent with Eq. (2), the energy variable U defined in Eq. (10) can be approximated by (with $p_r^2 << \gamma_0^2 m^2 c^2$)

$$U \simeq p_r^2/2\gamma_0 m + \psi_0(r) + \gamma_0 mc^2 \quad , \tag{11}$$

where

$$\psi_0(r) = [\gamma(r) - \gamma_0]mc^2 - \delta\phi_0(r) \tag{12}$$

is the "envelope function", and

$$\gamma(r)mc^2 = \{m^2c^4 + [c^2P_0/r + (e/c)A_0(r)]^2\}^{1/2} \quad , \tag{13}$$

is the electron energy associated with the azimuthal motion. Moreover, $\delta\phi_0(r)$ is defined by $\delta\phi_0(r) = \phi_0(r) - \bar{\phi}_0$, and $\gamma_0 mc^2 = \gamma(r=R_0)mc^2$ is the azimuthal electron energy at $r=R_0$. The envelope function $\psi_0(r)$ can be further simplified for a thin E-layer satisfying Eqs. (2) and (3) by Taylor expanding Eq. (12) about the mean radius R_0. Retaining terms to quadratic order in

$$\rho = r - R_0 \quad , \tag{14}$$

and making use of equilibrium radial force balance[16,19] on an electron fluid element at $r=R_0$, we find

$$\psi_0(r) = \frac{1}{2}\gamma_0 m\omega_r^2\rho^2 \quad , \tag{15}$$

where

$$\omega_r^2 = \omega_c^2 + \omega_p^2(1 - \gamma_0^2 f)/\gamma_0^2 \tag{16}$$

is the radial betatron frequency, $\omega_p^2 = 4\pi n_e^0(R_0)e^2/\gamma_0 m$ is the plasma frequency-squared at $r=R_0$, and $\omega_c = eB_0/\gamma_0 mc$ is the electron cyclotron frequency. [See Refs. 16 and 19 for a detailed discussion of Eq. (15)].

Making use of Eqs. (11) and (15), several interesting properties can be deduced for the class of thin E-layer equilibria described by Eq. (8). For example, it is straightforward to show that the electron

density profile can be expressed as

$$n_e^0(r)=\int d^3p f_e^0(H,P_\theta,P_z)=n_0 \frac{R_0}{r} \Theta(a^2-\rho^2) \ , \tag{17}$$

where

$$a=[2(\hat{\gamma}-\gamma_0)c^2/\gamma_0\omega_r^2]^{1/2} \tag{18}$$

is the half-thickness of the E-layer. In obtaining Eq. (17), use has been made of $(\partial/\partial p_\theta)P_\theta=r$ and the identity

$$\int_0^\alpha dx(\alpha^2-x^2)^{-1/2}=\pi/2 \ . \tag{19}$$

Since the E-layer is assumed to be thin, we approximate $R_0/r\simeq 1$ in Eq. (17), and the electron density profile reduces to

$$n_e^0(r) = \begin{cases} n_0 \ , & |r-R_0|<a \ , \\ 0 \ , & \text{otherwise} \ . \end{cases} \tag{20}$$

Moreover, it is straightforward to show that the axial electron temperature profile can be expressed as

$$T_z^0(r)=\int d^3p(p_z^2/\gamma_0 m) f_e^0 \Big/ \int d^3p f_e^0 = \Delta^2/3\gamma_0 m=\text{const.}, \tag{21}$$

for $|r-R_0|<a$. The electron density and axial temperature profiles are illustrated in Fig. 2. Evidently, the equilibrium distribution function in Eq. (8) corresponds to a sharp-boundary density profile [Eq. (20)] with uniform axial temperature [Eq. (21)].

Finally, we conclude this section by noting that the spread in axial momentum in Eq. (8) yields a corresponding spread in total energy H. From Eqs. (10), (11), and (15), we express

$$H = \gamma_0 mc^2 - e\bar{\phi}_0 + \frac{p_z^2}{2\gamma_0 m} + \left\{ \frac{p_r^2}{2\gamma_0 m} + \frac{1}{2}\gamma_0 m\omega_r^2\rho^2 \right\} \ . \tag{22}$$

Within the context of Eq. (2), it is valid to approximate Eq. (22) by

$$H \simeq \gamma_0 mc^2 - e\bar{\phi}_0 + p_z^2/2\gamma_0 m \ . \tag{23}$$

It is evident from Eq. (8) that 2Δ is a measure of the total spread in axial momentum. Therefore, from Eq. (23), the total energy spread can be approximated by

$$\Delta E = \Delta^2/2\gamma_0 m \ . \tag{24}$$

III. ELECTROMAGNETIC STABILITY ANALYSIS

A. Linearized Vlasov-Maxwell Equations

In this section, we examine the linearized Vlasov-Maxwell equations for perturbations about a thin E-layer equilibrium described by Eq. (8). To determine stability properties, we adopt a normal-mode approach in which all perturbations are assumed to vary with time according to

$$\delta\psi(\underset{\sim}{x},t)=\hat{\psi}(\underset{\sim}{x})\exp\{-i\omega t\} \ ,$$

with $\mathrm{Im}\omega>0$. Then the Maxwell equations for the perturbed electric and magnetic fields become[16]

$$\begin{aligned} \nabla\times\hat{\underset{\sim}{E}}(\underset{\sim}{x}) &= i\,\frac{\omega}{c}\,\hat{\underset{\sim}{B}}(\underset{\sim}{x}) \ , \\ \nabla\times\hat{\underset{\sim}{B}}(\underset{\sim}{x}) &= \frac{4\pi}{c}\,\underset{\sim}{J}(\underset{\sim}{x}) - i\,\frac{\omega}{c}\,\hat{\underset{\sim}{E}}(\underset{\sim}{x}) \ , \end{aligned} \tag{25}$$

where

$$\hat{\underset{\sim}{J}}(\underset{\sim}{x})=-e\int d^3p\ \underset{\sim}{v}\ \hat{f}_e(\underset{\sim}{x},\underset{\sim}{p}) \tag{26}$$

is the perturbed current density,

$$\hat{f}_e(\underset{\sim}{x},\underset{\sim}{p}) = e\int_{-\infty}^{0} d\tau\exp\{-i\omega\tau\}\left\{\hat{\underset{\sim}{E}}(\underset{\sim}{x}') + \frac{\underset{\sim}{v}'\times\hat{\underset{\sim}{B}}(\underset{\sim}{x}')}{c}\right\}\cdot\frac{\partial}{\partial\underset{\sim}{p}'}\,f_e^0 \tag{27}$$

is the perturbed distribution function, and $\tau\equiv t'-t$. To make the theoretical analysis tractable, we Fourier decompose the θ- and z-dependence of all perturbed quantities according to

$$\hat{\psi}(\underset{\sim}{x})=\sum_{\ell}\int dk\,\hat{\psi}_\ell(k,r)\exp\{i(\ell\theta+kz)\} \ , \tag{28}$$

where k is the axial wavenumber and ℓ is an integer. Making use of

Eqs. (25) and (28), it is straightforward to show that

$$\frac{\partial}{\partial r}\hat{B}_{\ell z}(k,r) - \frac{c\ell^2}{r\omega}p^2\left(\hat{\phi}(r) + \frac{ik}{p^2}\hat{E}_{\ell z}(k,r)\right) = -\frac{4\pi}{c}\hat{J}_{\ell\theta}(k,r) , \tag{29}$$

where

$$p^2=\omega^2/c^2-k^2 \tag{30}$$

and the function $\hat{\phi}(r)$ is defined by

$$\hat{\phi}(r)=ir\hat{E}_{\ell\theta}(k,r)/\ell . \tag{31}$$

Equation (29) can be expressed as

$$\frac{\partial}{\partial r}\hat{B}_{\ell z}(k,r) = \frac{c\ell^2p^2}{r\omega}\left(\hat{\phi}(r) + \frac{ik}{p^2}\hat{E}_{\ell z}(k,r)\right) \tag{32}$$

outside the E-layer, because the perturbed azimuthal current density $\hat{J}_{\ell\theta}(k,r)=0$ in the vacuum region.

The perturbed axial and azimuthal electric fields [$\hat{E}_{\ell z}(k,r)$ and $\hat{E}_{\ell\theta}(k,r)$] are continuous across the beam boundaries ($r=R_1$ and $r=R_2$), as is the function $\hat{\phi}(r)$ [Eq. (31)]. Integrating Eq. (29) from $r=R_1-\delta$ to $r=R_2+\delta$ and taking the limit $\delta\to 0_+$, we obtain

$$\hat{B}_{\ell z}(k,R_2^+)-\hat{B}_{\ell z}(k,R_1^-) = -\frac{4\pi}{c}\chi(\omega)\hat{\phi}(R_0) + \frac{c\ell}{\omega}p^2\int_{R_1}^{R_2}dr\left(\hat{\phi}(r)/r + \frac{ik}{p^2r}\hat{E}_{\ell z}(k,r)\right) , \tag{33}$$

where the effective susceptibility[16] is defined by

$$\chi(\omega)\hat{\phi}(R_0)=\int_{R_1^-}^{R_2^+}dr\, J_{\ell\theta}(r) , \tag{34}$$

and $\psi(R_j^+)$ denotes $\lim_{\delta\to 0_+}\psi(R_j+\delta)$. For present purposes, it is also

assumed that

$$|\omega - \ell\omega_c| << \omega_r \ ,$$

$$\ell(\omega_c/\omega_r) << R_0/a \ . \tag{35}$$

Within the context of assumption (d) and Eq. (35), it is valid to approximate[14,16]

$$\hat{\phi}(r) \simeq \hat{\phi}(R_0) \ ,$$

$$\hat{E}_{\ell z}(k,r) \simeq \hat{E}_{\ell z}(k,R_0) \ , \tag{36}$$

$$\hat{B}_{\ell\theta}(k,r) \simeq \hat{B}_{\ell\theta}(k,R_0) \ .$$

For convenience, in the subsequent analysis we introduce the normalized electric and magnetic wave admittances,[14,16] $d_\pm$ and $b_\pm$, defined at the inner and outer surfaces of the E-layer by

$$d_+ = -[r(\partial/\partial r)\hat{E}_{\ell z}(k,r)]_{R_2^+} \Big/ [\ell \hat{E}_{\ell z}(k,R_2)] \ ,$$

$$d_- = [r(\partial/\partial r)\hat{E}_{\ell z}(k,r)]_{R_1^-} \Big/ [\ell \hat{E}_{\ell z}(k,R_1)] \ , \tag{37}$$

and

$$b_+ = -\ell\hat{B}_{\ell z}(k,R_2^+) / [r(\partial/\partial r)\hat{B}_{\ell z}(k,r)]_{R_2} \ ,$$

$$b_- = \ell\hat{B}_{\ell z}(k,R_1^-) / [r(\partial/\partial r)\hat{B}_{\ell z}(k,r)]_{R_1} \ . \tag{38}$$

For a beam in vacuum, the values of $b_\pm$ and $d_\pm$ depend on the geometric configuration (Appendix). Making use of Eqs. (32)-(38), it is straightforward to show that

$$(b_- + b_+)[\hat{\phi}(R_0) + ik\hat{E}_{\ell z}(k,R_0)/p^2] = \frac{4\pi\omega}{c^2 p^2}\chi(\omega)\hat{\phi}(R_0) \ . \tag{39}$$

Fourier-decomposing the perturbed fields in Eq. (25), we obtain

$$\hat{B}_{\ell\theta}(k,r) = -\frac{k\ell}{p^2 r}\hat{B}_{\ell z}(k,r) + \frac{i\omega}{cp^2}\frac{\partial}{\partial r}\hat{E}_{\ell z}(k,r) \tag{40}$$

in the vacuum region. Since $\hat{B}_{\ell\theta}(k,r)$ is continuous across the beam boundaries and approximately constant within the beam (Eq. (36)], it is straightforwrad to show from Eq. (40) that

$$i\frac{\omega}{k\ell c}\{[r(\partial/\partial r)\hat{E}_{\ell z}(k,r)]_{R_2^+} - [r(\partial/\partial r)\hat{E}_{\ell z}(k,r)]_{R_1^-}\}$$
$$= \hat{B}_{\ell z}(k,R_2^+) - \hat{B}_{\ell z}(k,R_1^-) \ . \tag{41}$$

Substituting Eqs. (33) and (37) into Eq. (41), and making use of Eq. (35), we find

$$(d_- + d_+)\hat{E}_{\ell z}(k,R_0) = -i\frac{4\pi k}{\omega}\chi(\omega)\hat{\phi}(R_0) \ . \tag{42}$$

After some simple algebraic manipulation that makes use of Eqs. (39) and (42), the function $\hat{\phi}(R_0)$ can be expressed as

$$\frac{2\pi}{\omega} g\chi(\omega) = 1 \ , \tag{43}$$

where the geometric factor g is defined by

$$g = \frac{2}{p^2}\left(\frac{\omega^2/c^2}{b_- + b_+} - \frac{k^2}{d_- + d_+}\right) \ . \tag{44}$$

Evidently, an evaluation of the effective susceptibility $\chi(\omega)$ is required for a detailed stability analysis.

B. Effective Susceptibility

In this section, we evaluate the perturbed azimuthal current density, and the effective susceptibility $\chi(\omega)$ defined in Eq. (34).

From the Maxwell equation $\nabla\times\hat{\mathbf{E}}(\mathbf{x})=i(\omega/c)\hat{\mathbf{B}}(\mathbf{x})$, we obtain

$$\hat{E}_{\ell z}(k,r) - \frac{r\omega}{\ell c}\hat{B}_{\ell r}(k,r)=-ik\hat{\phi}(r) ,$$

$$\hat{E}_{\ell r}(k,r) + \frac{r\omega}{\ell c}\hat{B}_{\ell z}(k,r) = -\frac{\partial}{\partial r}\hat{\phi}(r) . \tag{45}$$

Since the eigenfrequency for the negative-mass instability is given approximately by $\omega\simeq\ell\omega_c$ for $V_z^0(r)=0$, and since the thickness of E-layer is much smaller than its major radius, Eq. (45) can be approximated by

$$\hat{E}_{\ell z}(k,r)-(v_\theta/c)\hat{B}_{\ell r}(k,r)=-ik\hat{\phi}(r) ,$$

$$\hat{E}_{\ell r}(k,r)+(v_\theta/c)\hat{B}_{\ell z}(k,r)=-(\partial/\partial r)\hat{\phi}(r) . \tag{46}$$

After some straightforward algebra that makes use of Eqs. (27) and (46), we obtain

$$\hat{f}_{e\ell}(\mathbf{x},\mathbf{p})=-e\int_{-\infty}^{0} d\tau\, \exp\{-i\omega\tau\}\nabla'\hat{\phi}(\mathbf{x}')\cdot\frac{\partial}{\partial\mathbf{p}'}f_e^0(H,P_\theta,P_z) , \tag{47}$$

where $\hat{\phi}(\mathbf{x})=\hat{\phi}(r)\exp\{i(\ell\theta+kz)\}$, and leading-order terms have been retained [see Eq. (35)]. Fourier decomposing Eq. (47) according to Eq. (28) and making use of the approximation $\hat{\phi}(r)\simeq\hat{\phi}(R_0)$ [Eq. (36)], the perturbed distribution function can be expressed as

$$\hat{f}_{e\ell}(r,\mathbf{p})=-ie\hat{\phi}(R_0)I[k(\partial/\partial P_z)+\ell(\partial/\partial P_\theta)]f_e^0(H,P_\theta P_z) , \tag{48}$$

where the orbit integral I is defined by

$$I=\int_{-\infty}^{0} d\tau\, \exp\{i[\ell(\theta'-\theta)+k(z'-z)-\omega\tau]\} . \tag{49}$$

As indicated in Eq. (49), the particle trajectories, $\theta'(\tau)$ and

$z'(\tau)$, in the equilibrium fields are required in order to evaluate the orbit integral I. Making use of the Hamiltonian in Eq. (5), it is straightforward to obtain the equations of motion. Assuming that the electron orbit passes through the phase-space point (z,p_z) and $\theta'=\theta$ at time $t'=t$, we find

$$z'=z+p_z\tau/\gamma_0 m \ ,$$

$$\theta'=\theta+(\omega_c-\mu\delta P_\theta/\gamma_0 m R_0^2)\tau \ , \tag{50}$$

where

$$\mu=\omega_c^2/\omega_r^2-1/\gamma_0^2 \ , \tag{51}$$

and $\delta P_\theta=P_\theta-P_0$. [See Ref. 16 for a detailed derivation of Eq. (50)]. Substituting Eq. (50) into Eq. (49), we obtain

$$I=i(\omega-\ell\omega_c-kp_z/\gamma_0 m+\mu\ell\delta P_\theta/\gamma_0 m R_0^2)^{-1} \ . \tag{52}$$

From Eq. (26), the perturbed azimuthal current density can be expressed as

$$\hat{J}_{\ell\theta}(k,r)=-e\omega_c R_0\int d^3p \ \hat{f}_{e\ell}(r,p) \ , \tag{53}$$

where we have approximated $v_\theta\simeq R_0\omega_c$ for a thin, relativistic E-layer. Substituting Eqs. (48) and (52) into Eq. (53), and carrying out the momentum integration, the perturbed azimuthal current density can be expressed as

$$\hat{J}_{\ell\theta}(k,r) = -\hat{\phi}(R_0)\frac{e^2 n_0\omega_c}{\gamma_0 m R_0}\frac{\mu\ell^2-k^2R_0^2}{(\omega-\ell\omega_c)^2-k^2\Delta^2/\gamma_0^2m^2} \ , \tag{54}$$

where use has been made of $a<<R_0$. The number of electrons per unit axial length of the E-layer (N_e) can be determined by substituting

Eq. (17) into Eq. (4). Within the context of Eq. (2), we obtain the approximate result $N_e = 4\pi a n_0 R_0$. Eliminating n_0 in favor of N_e in Eq. (54) and substituting Eq. (54) into Eq. (34) gives

$$\chi(\omega) = -\frac{N_e e^2 \omega_c}{2\pi \gamma_0 m R_0^2} \frac{\mu \ell^2 - k^2 R_0^2}{(\omega - \ell\omega_c)^2 - k^2 \Delta^2/\gamma_0^2 m^2} . \tag{55}$$

Equation (55) is used in Sec. IV to complete the stability analysis.

IV. NEGATIVE-MASS STABILITY PROPERTIES

Substituting Eq. (55) into Eq. (43) and making use of Eq. (24) and the definition of Budker's parameter, $\nu=N_e e^2/mc^2$, the dispersion relation for the negative-mass instability can be expressed as

$$(\omega-\ell\omega_c)^2 = -\frac{c^2}{R_0^2}\left(\frac{\nu}{\gamma_0}\frac{g\omega_c}{\omega}(\mu\ell^2-k^2R_0^2) - 2k^2R_0^2\frac{\Delta E}{\gamma_0 mc^2}\right) \tag{56}$$

for $1\leq\ell<R_0/a$. In Eq. (56), g is the geometric factor defined in Eq. (44), $\Delta E=\Delta^2/2\gamma_0 m$ is the energy spread [Eq. (21)], and $\mu=\omega_c^2/\omega_r^2-1/\gamma_0^2$ [Eq. (51)]. It should be noted that Eq. (56) is valid only when $|\omega-\ell\omega_c|<<\omega_r$ [Eq. (35)]. The growth rate $\omega_i=\text{Im}\omega$ and real oscillation frequency $\Omega_r=\text{Re}\omega$ can be determined from Eq. (56) for a broad range of parameters k, ν/γ_0 and $\alpha=\Delta E/\gamma_0 mc^2$, by solving numerically the full transcendental dispersion relation. [Note that the geometric factor g in Eq. (56) is generally a complicated function of the complex eigenfrequency ω.]

For present purposes, to illustrate the influence of the axial energy spread on the negative-mass instability, we calculate the normalized electric and magnetic wave admittances defined in Eqs. (A.3) and (A.4) by approximating $\omega\simeq\ell\omega_c$ in the expressions for $d_\pm$ and $b_\pm$. Figure 3 is a plot of sum of the wave admittances (b_-+b_+) and (d_-+d_+) versus normalized axial wavenumber kR_0, for $\ell=6$, $\gamma_0=5$, $a/R_0=0.02$, $T_0/R_0=1.5$, and $T_i=0$ (no inner conductor). In Fig. 3, the solid and broken curves correspond to (b_-+b_+) and (d_-+d_+), respectively. Evidently (b_-+b_+) and (d_-+d_+) are slowly varying functions of kR_0 for the range $0\leq kR_0\lesssim 2$, where the approximation $\omega\simeq\ell\omega_c$ is certainly valid. Negative-mass stability properties are illustrated in Figs. 4 and 5 for the range of axial wavenumbers $0\leq kR_0\lesssim 2$. Generally speaking, the quantities (b_-+b_+) and (d_-+d_+)

either vanish or become infinite at certain values of k. [For example, from Fig. 3, $(b_-+b_+)=0$ at $kR_0\simeq 3.1$, and $(b_-+b_+)\to\infty$ at $kR_0\simeq 3.5$.] Normal modes with axial wavenumber k for which $(b_-+b_+)\to 0$ or $(d_-+d_+)\to 0$, are purely transverse electric (TE) or transverse magnetic (TM) waveguide modes, respectively. The dispersion relation [Eq. (56)] for the purely TE and TM modes will be investigated elsewhere.[18]

Figure 4 shows a plot of normalized growth rate ω_i/ω_c versus kR_0 obtained from Eq. (56) for $f=0.1$, $\nu/\gamma_0=0.02$, several values of $\alpha=\Delta E/\gamma_0 mc^2$, and parameters otherwise similar to Fig. 3. Two important features are evident from Fig. 4. First, the axial energy spread stabilizes perturbations with axial wavenumber larger than a certain critical value. For example, perturbations with $kR_0>1.03$ are completely stabilized by a 4% energy spread ($\alpha=0.04$ in Fig. 4). Second, for given $kR_0\neq 0$, the growth rate can be substantially reduced by increasing the energy spread. These results are consistent with recent experimental observations by Destler et al.,[8] who find that a finite-length E-layer (in which kR_0 is necessarily nonzero) is stable whenever the energy spread is increased by a sufficiently large amount.

Stability boundaries in the parameter space $(kR_0,\ \Delta E/\gamma_0 mc^2)$ are illustrated in Fig. 5. The solid curves correspond to the stability boundaries ($\omega_i=0$) obtained from Eq. (56) for several values of ν/γ_0 and parameters otherwise similar to Figs. 3 and 4. For a given value of ν/γ_0, the region of $(kR_0,\ \Delta E/\gamma_0 mc^2)$ parameter space <u>above</u> the curve corresponds to stability ($\omega_i=0$), whereas the region of parameter space <u>below</u> the curve corresponds to instability ($\omega_i>0$). For sufficiently low beam density ($\nu/\gamma_0=0.01$, say), it is evident from Fig. 5 that the system is stable provided $kR_0\gtrsim 1$ and $\alpha\gtrsim 0.02$. However, even for low

beam densities, it is evident from Fig. 5 that long wavelength perturbations with $kR_{0} \lesssim 0.5$ are not stabilized by an axial energy spread, at least for the choice of distribution function in Eq. (8). In this regard, we hasten to point out that high-harmonic perturbations with small axial wavenumber can be stabilized by a spread in canonical angular momentum.[16]

We conclude this section by noting that stability properties also exhibit a sensitive dependence on the location of the conducting walls.[18] Moreover, the equilibrium and stability analysis presented here can be extended in a straightforward manner to hollow electron beams that propagate along the z-axis with a nonzero axial velocity $v_{z}^{0}\hat{e}_{z}$.

V. SUMMARY AND CONCLUSIONS

In this paper, we have examined the influence of axial energy spread on the negative-mass instability in a relativistic nonneutral E-layer. The analysis was carried out within the framework of a linearized Vlasov-Maxwell equation. The equilibrium (Sec. II) and negative-mass stability (Secs. III and IV) properties were investigated in detail for the choice of distribution function in which all electrons have the same value of canonical angular momentum and a step-function distribution in axial momentum p_z [Eq. (8)]. A detailed numerical analysis of the dispersion relation [Eq. (56)] was presented in Sec. IV. One of the most important conclusions of this study is that an axial energy spread can have a large influence on stability behavior. *In particular, perturbations with sufficiently* large axial wavenumber ($kR_{0\hat{z}} \gtrsim 1$) can be completely stabilized by a small axial energy spread $\Delta E \neq 0$. Moreover, in the special limiting case when $\Delta E = 0$ and $\mu = 1$, the stability properties are consistent with the results previously obtained by Briggs and Neil.[14]

Finally, we emphasize that the numerical analysis presented in Sec. IV is based on the assumption that the geometric factor g is a slow varying function of k. Although this is a reasonable approximation for $0 \leq kR_{0\hat{z}} \leq 2$ [Fig. 3], we expect significant modifications to the stability behavior whenever $(b_- + b_+) \to 0$ or $(d_- + d_+) \to 0$. The excitation of transverse electric $[(b_- + b_+) \to 0]$ and transverse magnetic $[(d_- + d_+) \to 0]$ waveguide modes by the negative-mass instability is currently under investigation.[18]

ACKNOWLEDGMENTS

It is a pleasure to acknowledge the benefit of useful discussions with Dr. Hogil Kim.

This research was supported by the National Science Foundation. The research by one of the authors (H.U.) was supported in part by the Office of Naval Research under the auspices of the University of Maryland-Naval Research Laboratory Joint Program in Plasma Physics.

APPENDIX

WAVE ADMITTANCE AT THE BOUNDARIES OF AN E-LAYER IN A CYLINDRICAL CAVITY

In this section, we obtain expressions for the wave admittances at the boundaries of an E-layer in a cylindrical cavity. Since the perturbed current density vanishes in the vacuum regions outside the E-layer, the Maxwell equations in this region can be expressed as

$$\left(\frac{1}{r}\frac{\partial}{\partial r}\, r\, \frac{\partial}{\partial r} - \frac{\ell^2}{r^2} + p^2\right) \begin{Bmatrix} \hat{E}_{\ell z}(k,r) \\ \\ \hat{B}_{\ell z}(k,r) \end{Bmatrix} = 0 \tag{A.1}$$

In obtaining Eq. (A.1), use has been made of Eqs. (25), (28) and (30). The solution to Eq. (A.1) is given by

$$\begin{Bmatrix} \hat{E}_{\ell z}(k,r) \\ \hat{b}_{\ell z}(k,r) \end{Bmatrix} = \begin{cases} AJ_\ell(pr)+BN_\ell(pr) \ , & R_2 < r < T_0 \ , \\ CJ_\ell(pr)+DN_\ell(pr) \ , & T_i < r < R_1 \ , \end{cases} \tag{A.2}$$

where $J_\ell(pr)$ and $N_\ell(pr)$ are Bessel functions of the first and second kind, respectively, and T_i and T_0 are the radii of the inner and outer conductors, respectively (see Fig. 1). In Eq. (A.2), A, B, C and D are constants which are determined from Eqs. (37) and (38) and the boundary conditions for the perturbed fields.

Making use of the boundary conditions $\hat{E}_{\ell z}(k,T_i)=\hat{E}_{\ell z}(k,T_0)=0$, the electric wave admittances at the inner and outer boundaries of E-layer [Eq. (37)] can be expressed as

$$\begin{aligned} d_+ &= -\frac{R_2 p}{\ell}\, \frac{J'_\ell(pR_2)N_\ell(pT_0)-J_\ell(pT_0)N'_\ell(pR_2)}{J_\ell(pR_2)N_\ell(pT_0)-J_\ell(pT_0)N_\ell(pR_2)} \ , \\ d_- &= \frac{R_1 p}{\ell}\, \frac{J'_\ell(pR_1)N_\ell(pT_i)-J_\ell(pT_i)N'_\ell(pR_1)}{J_\ell(pR_1)N_\ell(pT_i)-J_\ell(pT_i)N_\ell(pR_1)} \ , \end{aligned} \tag{A.3}$$

where the prime (') denotes $(1/p)(d/dr)$, $p=(\omega^2/c^2-k^2)^{1/2}$, and R_1 and R_2 are the inner and outer radii of the E-layer. Similarly, the magnetic wave admittances at the inner and outer boundaries of the E-layer [Eq. (38)] can be expressed as

$$b_+ = -\frac{\ell}{R_2 p}\frac{J_\ell(pR_2)N'_\ell(pT_0)-J'_\ell(pT_0)N_\ell(pR_2)}{J'_\ell(pR_2)N'_\ell(pT_0)-J'_\ell(pT_0)N'_\ell(pR_2)}\,,$$

$$b_- = \frac{\ell}{R_1 p}\frac{J_\ell(pR_1)N'_\ell(pT_i)-J'_\ell(pT_i)N_\ell(pR_1)}{J'_\ell(pR_1)N'_\ell(pT_i)-J'_\ell(pT_i)N'_\ell(pR_1)}\,, \tag{A.4}$$

where use has been made of the boundary conditions $[(\partial/\partial r)\hat{B}_{\ell z}(k,r)]_{T_i} = [(\partial/\partial r)\hat{B}_{\ell z}(k,r)]_{T_0}=0$.

REFERENCES

1. D. M. Woodall, H. H. Fleischmann, and H. L. Berk, Phys. Rev. Lett. 34, 260 (1975).
2. H. A. Davis, R. A. Meger, and H. H. Fleischmann, Phys. Rev. Lett. 37, 542 (1976).
3. C. M. Armstrong, D. A. Hammer, and A. W. Trivelpiece, Phys. Lett. 55A, 413 (1976).
4. C. A. Kapetanakos, R. E. Pechacek, D. M. Spero, and A. W. Trivelpiece, Phys. Fluids 14, 155 (1971).
5. W. W. Destler, D. W. Hudgings, R. A. Kehs, P. K. Misra, and M. J. Rhee, IEEE Trans. NS-22, 995 (1975).
6. U. Schumacher, C. Andelfinger, and M. Ulrich, IEEE Trans. NS-22, 989 (1975).
7. S. Kawasaki, N. Kobayashi, Y. Kubota, and A. Migahara, IEEE Trans. NS-22, 992 (1975).
8. W. W. Destler, D. W. Hudgings, M. J. Rhee, S. Kawasaki, and V. L. Granatstein, J. Appl. Phys., in press (1977).
9. A. Faltens, G. R. Lambertson, J. M. Peterson, and J. B. Rechen, Proc. IXth Int. Conf. on High Energy Accelerators, 226 (Stanford, Calif., 1974).
10. C. H. Dustmann, W. Heinz, H. Krauth, L. Steinbock, and W. Zernial, Proc. IXth Int. Conf. on High Energy Accelerators, 250 (Stanford, Calif., 1974).
11. J. Fink, W. Herrmann, W. Ott, and J. M. Peterson, Proc. IXth Int. Conf. on High Energy Accelerators, 223 (Stanford, Calif., 1974).
12. R. W. Landau and V. K. Neil, Phys. Fluids 9, 2412 (1966).
13. V. K. Neil and W. Heckrotte, J. Appl. Phys. 36, 2761 (1966).

14. R. J. Briggs and V. K. Neil, Plasma Phys. 9, 209 (1967).

15. Y. Y. Lau and R. J. Briggs, Phys. Fluids 14, 967 (1971).

16. H. Uhm and R. C. Davidson, Phys. Fluids 20, 771 (1977).

17. R. C. Davidson, Theory of Nonneutral Plasmas, (W. A. Benjamin, Reading, Mass., 1974).

18. "Intense Microwave Generation by the Negative-Mass Instability", H. Uhm and R. C. Davidson, manuscript in preparation (1977).

19. R. C. Davidson and S. Mahajan, Phys. Fluids 17, 2090 (1974).

FIGURE CAPTIONS

Fig. 1 Equilibrium configuration and coordinate system.

Fig. 2 Electron density [Eq. (20)] and axial temperature profiles [Eq. (21)].

Fig. 3 Plot of sum of wave admittances (b_-+b_+) and (d_-+d_+) (Appendix) versus normalized axial wavenumber kR_0, for $\ell=6$, $\gamma_0=5$, $a/R_0=0.02$, $T_0/R_0=1.5$ and $T_i=0$.

Fig. 4 Plot of normalized growth rate ω_i/ω_c versus kR_0 [Eq. (56)], for $f=0.1$, $\nu/\gamma_0=0.02$, and several values of $\alpha=\Delta E/\gamma_0 mc^2$. Parameters are otherwise similar to Fig. 3.

Fig. 5 Stability boundaries [Eq. (56)] in the parameter space $(kR_0, \Delta E/\gamma_0 mc^2)$ for several values of ν/γ_0 and parameters otherwise similar to Figs. 3 and 4.

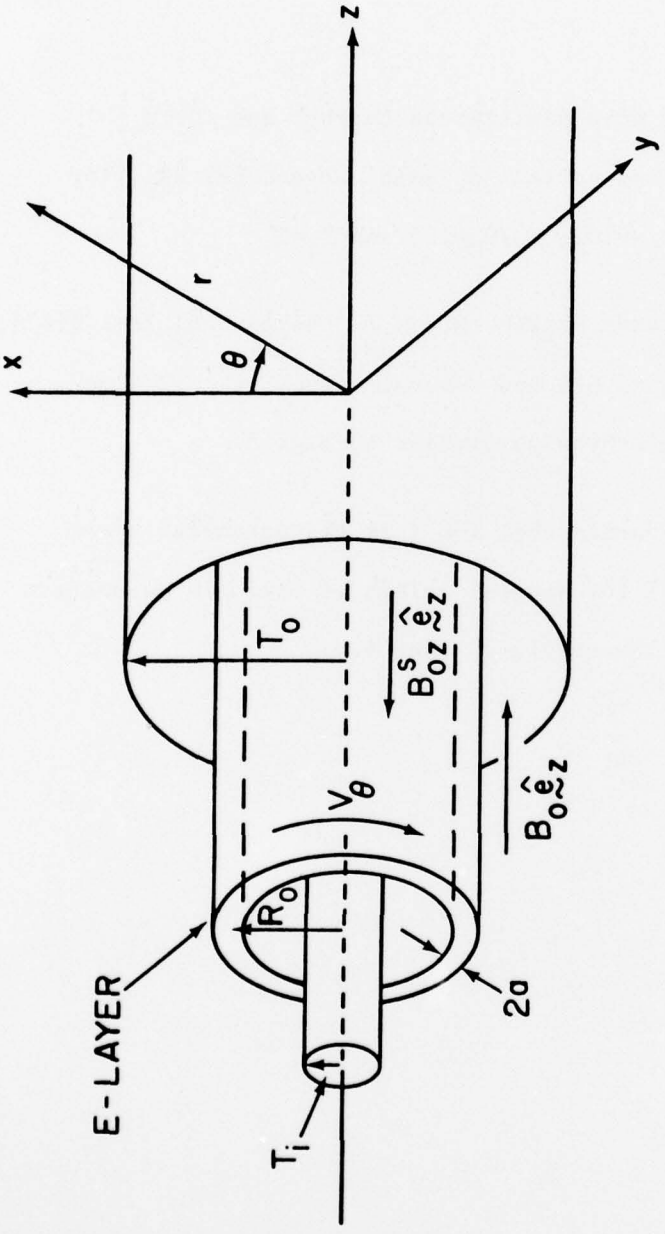

Fig. 1

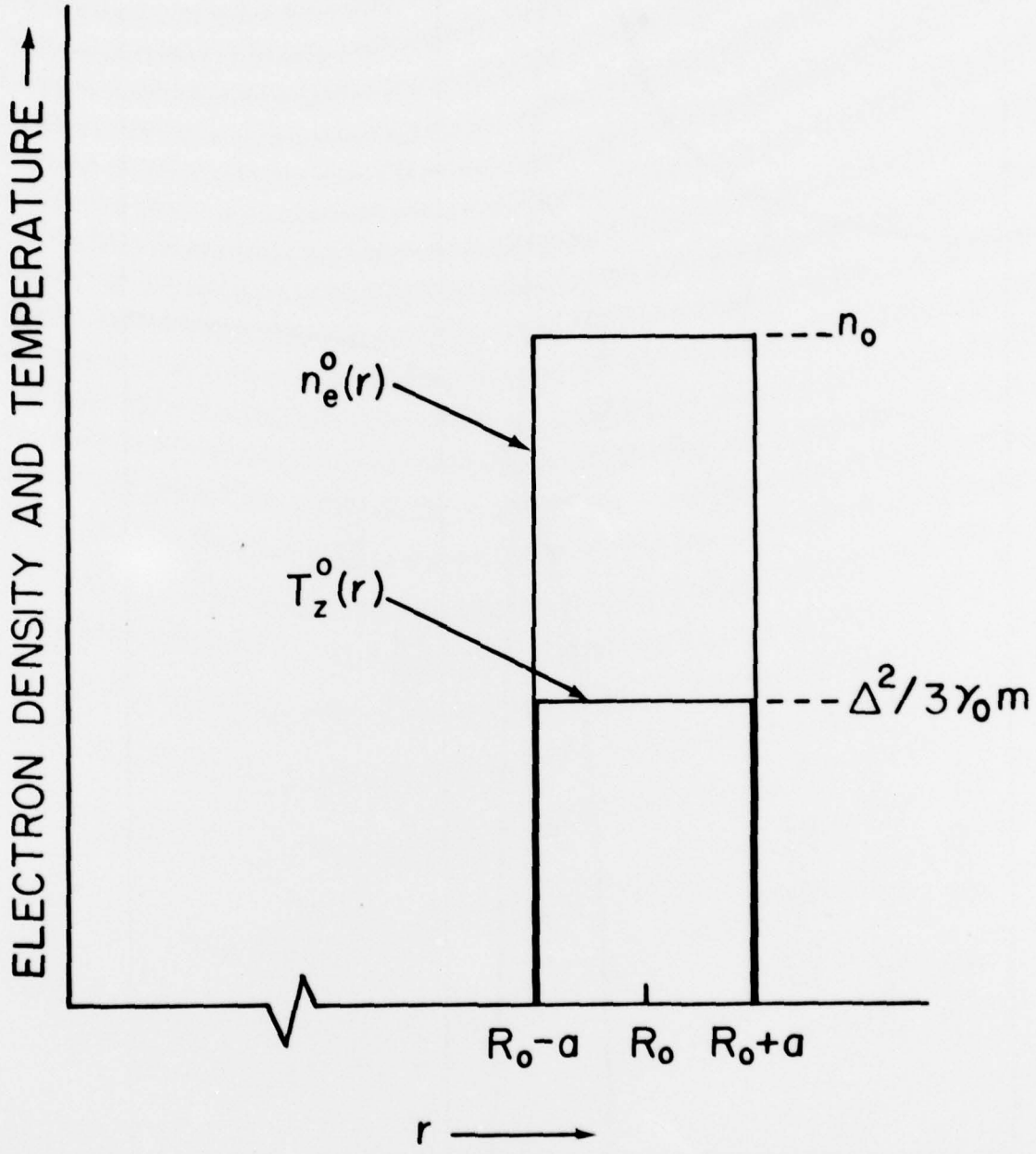
ELECTRON DENSITY AND TEMPERATURE →
$n_e^o(r)$
$T_z^o(r)$
n_o
$\Delta^2/3\gamma_o m$
R_o-a
R_o
R_o+a
r →

Fig. 2

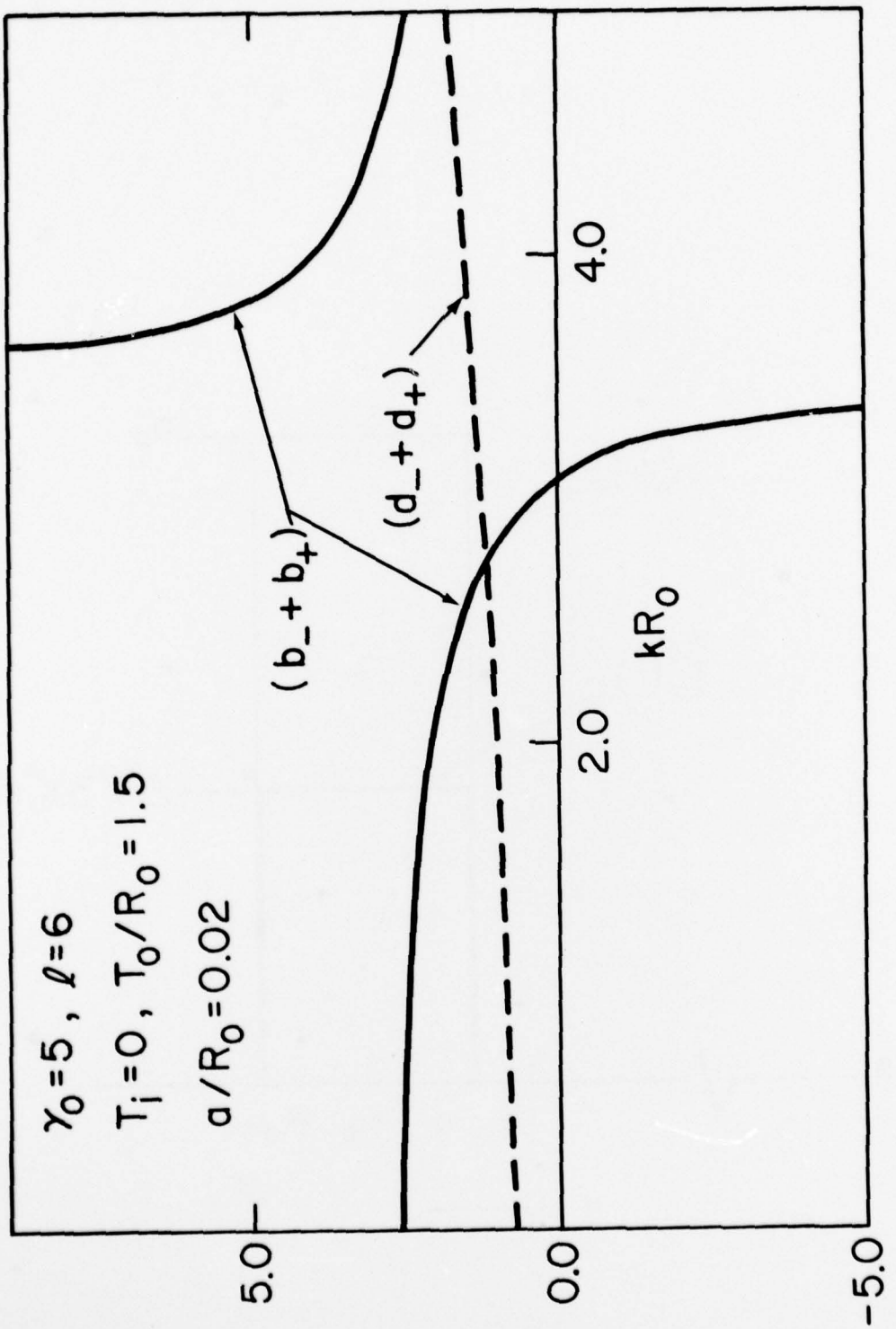

Fig. 3

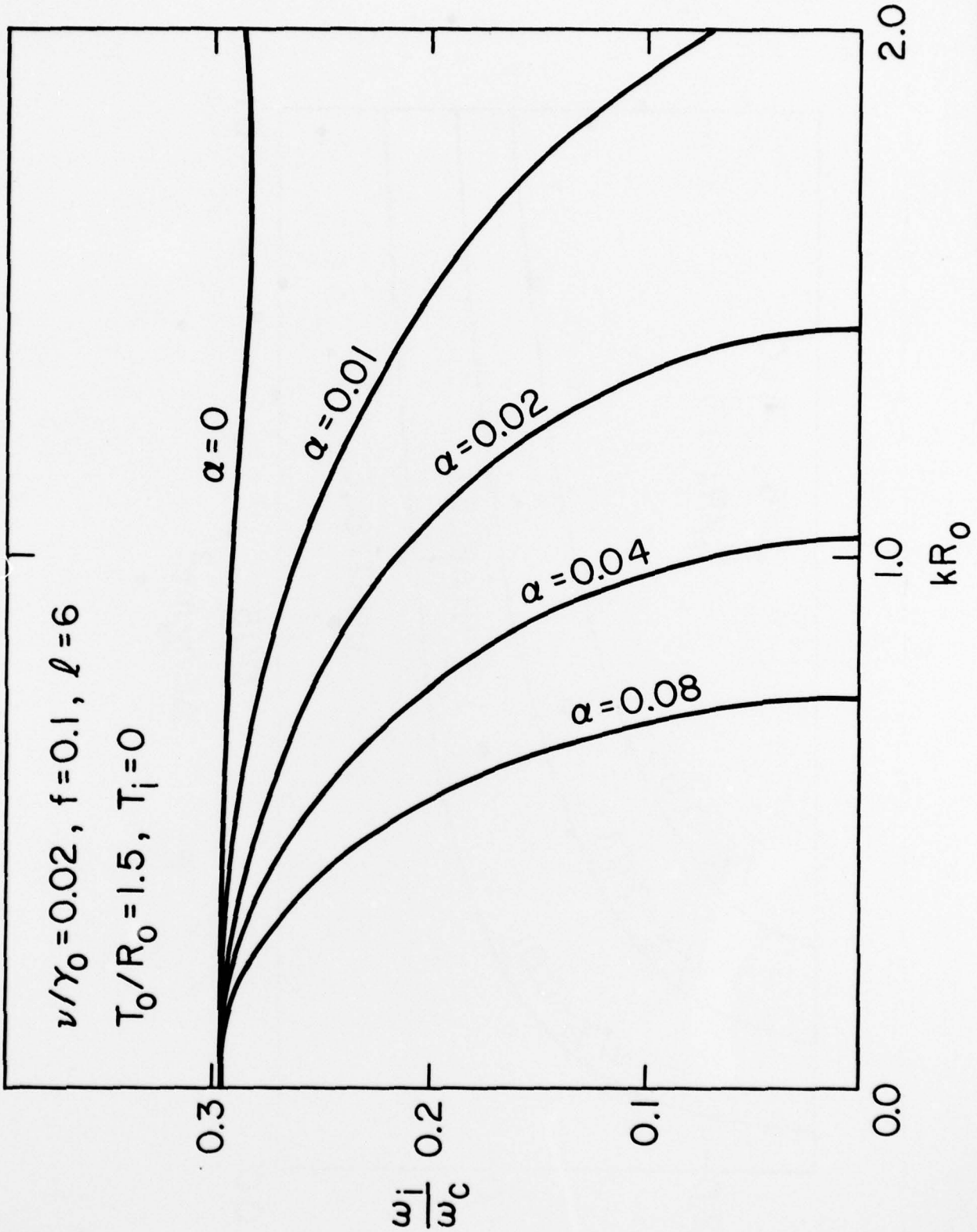
$\nu/\gamma_0=0.02$, f=0.1, $\ell=6$
$T_0/R_0=1.5$, $T_i=0$
α=0
α=0.01
α=0.02
α=0.04
α=0.08
0.3
0.2
0.1
0.0
$\frac{\omega_i}{\omega_c}$
1.0
2.0
kR_0

Fig. 4

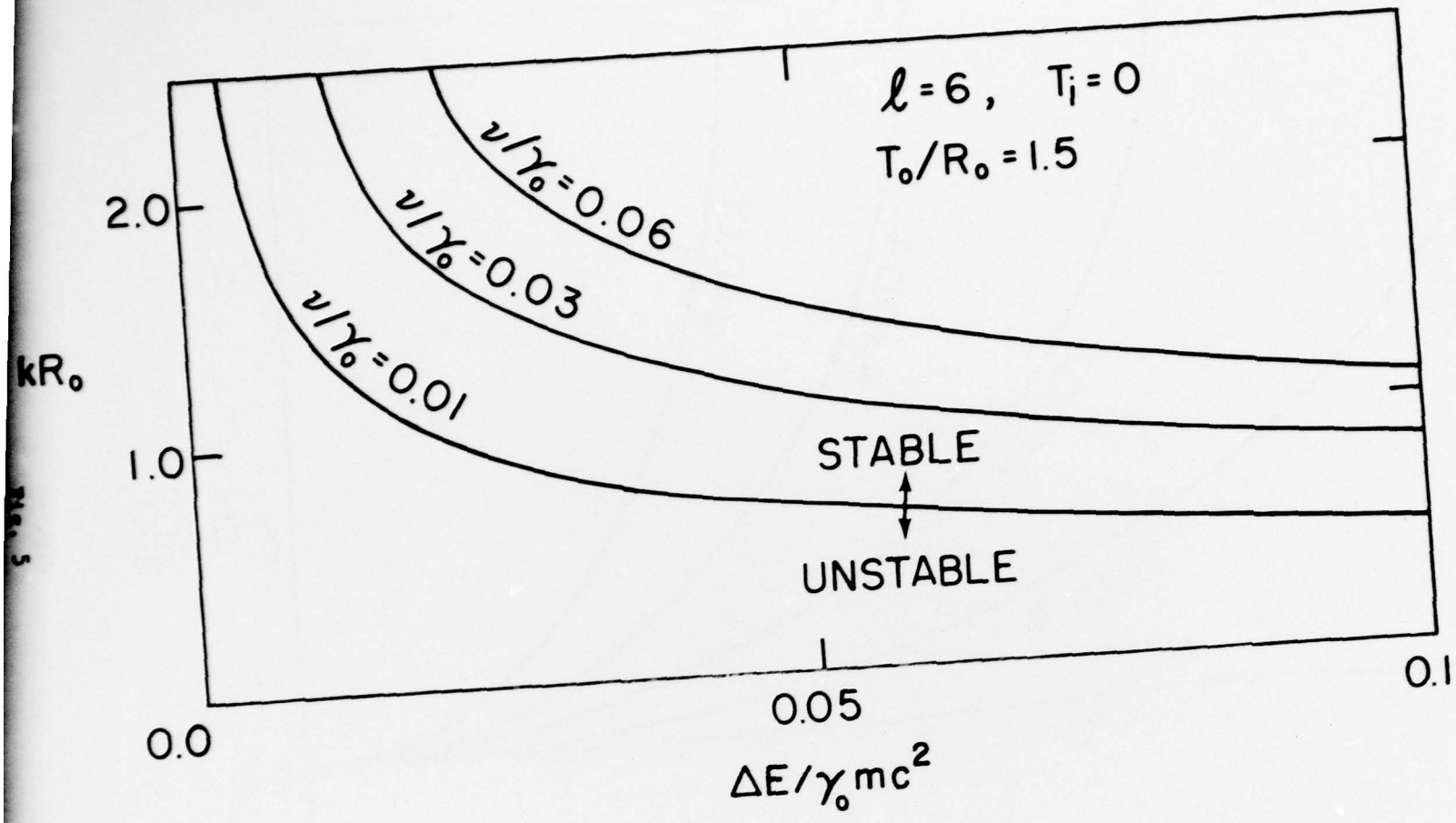
$\ell = 6, \quad T_i = 0$
$T_0/R_0 = 1.5$
$\nu/\gamma_0 = 0.06$
$\nu/\gamma_0 = 0.03$
$\nu/\gamma_0 = 0.01$
STABLE
UNSTABLE
2.0
1.0
0.0
0.05
0.1
kR_0
$\Delta E/\gamma_0 mc^2$

Fig. 5